The Relationship Between Subcortical Brain Volume and Striatal Dopamine $D_{2/3}$ Receptor Availability in Healthy Humans Assessed With [^{11}C]-Raclopride and [^{11}C]-(+)-PHNO PET

Fernando Caravaggio,[1,2] Jun Ku Chung,[1] Eric Plitman,[1] Isabelle Boileau,[1,2] Philip Gerretsen,[1,2] Julia Kim,[1] Yusuke Iwata,[1,2] Raihaan Patel,[3,4] M. Mallar Chakravarty,[3,4,5] Gary Remington,[1,2] and Ariel Graff-Guerrero[1,2]*

[1]*Research Imaging Centre, Centre for Addiction and Mental Health, 250 College Street, Toronto, Ontario M5T 1R8, Canada*
[2]*Department of Psychiatry, University of Toronto, 250 College Street, Toronto, Ontario M5T 1R8, Canada*
[3]*Department of Biological & Biomedical Engineering, McGill University, Montreal, Quebec H4H 1R3, Canada*
[4]*Cerebral Imaging Centre, Douglas Mental Health Institute, McGill University, Montreal, Quebec H4H 1R3, Canada*
[5]*Department of Psychiatry, McGill University, Montreal, Quebec H4H 1R3, Canada*

Abstract: *Background:* Abnormalities in dopamine (DA) and brain morphology are observed in several neuropsychiatric disorders. However, it is not fully understood how these abnormalities may relate to one another. For such in vivo findings to be used as biomarkers for neuropsychiatric disease, it must be understood how variability in DA relates to brain structure under healthy conditions. We explored how the availability of striatal DA $D_{2/3}$ receptors ($D_{2/3}R$) is related to the volume of subcortical brain structures in a sample of healthy humans. Differences in $D_{2/3}R$ availability measured with an antagonist radiotracer ([^{11}C]-raclopride) versus an agonist radiotracer ([^{11}C]-(+)-PHNO) were examined. *Methods:* Data from 62 subjects scanned with [^{11}C]-raclopride (mean age = 38.98 ± 14.45; 23 female) and 68 subjects scanned with [^{11}C]-(+)-PHNO (mean age = 38.54 ± 14.59; 25 female) were used. Subcortical volumes were extracted from T1-weighted images using the Multiple Automatically Generated Templates (MAGeT-Brain) algorithm. Partial correlations were used controlling for age, gender, and total brain volume. *Results:* For [^{11}C]-(+)-PHNO, ventral caudate volumes were positively correlated with BP_{ND} in the dorsal caudate and globus pallidus (GP). Ventral striatum (VS) volumes were positively correlated with BP_{ND} in the VS. With [^{11}C]-raclopride, BP_{ND} in the VS was negatively correlated with subiculum volume of the hippocampus. Moreover, BP_{ND} in the GP was negatively correlated with the volume of the lateral posterior nucleus of the thalamus. *Conclusion:* Findings are purely exploratory and presented corrected and uncorrected for multiple comparisons. We hope they will help inform the

Additional Supporting Information may be found in the online version of this article.

*Correspondence to: Dr. Ariel Graff-Guerrero, Centre for Addiction and Mental Health, 80 Workman Way, 6th Floor, Toronto, ON M6J1H4, Canada. E-mail: ariel.graff@camh.ca

Received for publication 6 March 2017; Revised 21 June 2017; Accepted 16 July 2017.
DOI: 10.1002/hbm.23744
Published online 28 July 2017 in Wiley Online Library (wileyonlinelibrary.com).

interpretation of future PET studies where concurrent changes in $D_{2/3}R$ and brain morphology are observed. *Hum Brain Mapp 38:5519–5534, 2017.*

Key words: dopamine; positron emission tomography; $D_{2/3}$ receptors; raclopride; PHNO; morphology; volume; striatum

INTRODUCTION

Elucidating neurochemical and structural brain changes associated with mental disorders remains a critical challenge for the development of robust "biomarkers" in psychiatry [Perlis, 2011]. However, it remains poorly understood how in vivo differences in neurochemistry relates to variation in brain structure. For example, while it has been demonstrated that persons with schizophrenia have increased endogenous dopamine (DA) levels in the striatum [Abi-Dargham et al., 2000; Caravaggio et al., 2015b; Kegeles et al., 2010], this has yet to be associated with any of the morphological brain changes observed in this disorder [Ellison-Wright et al., 2008; Haijma et al., 2013; Rimol et al., 2010; Song et al., 2015; van Erp et al., 2016; Xiao et al., 2015]. Similarly in obesity, while changes in DA $D_{2/3}$ receptor ($D_{2/3}R$) availability [Caravaggio et al., 2015c; Dang et al., 2016; Gaiser et al., 2016; Guo et al., 2014; Karlsson et al., 2016; Mawlawi et al., 2001] and brain morphology [Bond et al., 2011; Taki et al., 2008; Veit et al., 2014; Walther et al., 2010] have been observed, these changes have yet to be directly associated with each other [Karlsson, 2016]. Thus, the use of in vivo DA functioning and brain morphology as biomarkers for disease remains hindered insofar as it is not firmly established how they may relate to one another under normal conditions [Strimbu and Tavel, 2010].

While several animal studies have examined the effect of altering DA levels on brain development [Alvarez et al., 2002; Jones et al., 1996; Kalsbeek et al., 1989; Meredith et al., 1995; Pappas et al., 1992; Reinoso et al., 1996], few human studies have examined how in vivo DA functioning, measured with positron emission tomography (PET), relates to brain morphology [Casey et al., 2013; Morales et al., 2015; Werhahn et al., 2006; Woodward et al., 2009]. Using voxel-based morphology and the antagonist radioligand [^{18}F]-fallypride, Woodward et al. were the first to examine how variations in brain morphology relates to $D_{2/3}R$ availability in healthy persons [Woodward et al., 2009]. They observed that $D_{2/3}R$ availability within a given brain region was generally positively correlated with the gray matter (GM) density/volume of that region (e.g., within the caudate, thalamus, amygdala, and substantia nigra). This generally suggests that, (i) $D_{2/3}R$ availability may vary positively with the amount of GM, and/or, (ii) differences in $D_{2/3}R$ availability may alter brain structure during development [Woodward et al., 2009]. However, negative correlations [Woodward et al., 2009], and null correlations [Werhahn et al., 2006], have been observed between hippocampal volume and hippocampal $D_{2/3}R$ availability measured with [^{18}F]-fallypride. Using [^{18}F]-fallypride, midbrain $D_{2/3}R$ availability was also found to be positively correlated with GM volume in the striatum, prefrontal cortex, insula, hippocampus, and temporal cortex of methamphetamine users, but not healthy controls [Morales et al., 2015]. Finally, using [^{11}C]-raclopride, it has been demonstrated that striatal DA release in response to amphetamine is negatively correlated with frontal lobe thickness in healthy controls [Casey et al., 2013].

Previous studies have not systematically examined how striatal $D_{2/3}R$ availability is related to subcortical morphology in healthy persons. Moreover, previous studies have only used antagonist radiotracers for $D_{2/3}R$, that is, [^{18}F]-fallypride and [^{11}C]-raclopride. It is generally believed that $D_{2/3}R$ exist in (at least) two conformational states for agonist binding: an active state (D_2High) and an inactive state (D_2Low) [Seeman, 2011]. In theory, agonist radiotracers—such as [^{11}C]NPA [Narendran et al., 2004], [^{11}C]MNPA [Finnema et al., 2005], and [^{11}C]-(+)-PHNO [Willeit et al., 2006]—should preferably bind to "active" $D_{2/3}R$. Thus, agonist radiotracers may provide a more sensitive and physiologically meaningful estimate of DA release and $D_{2/3}R$ availability, respectively.

[^{11}C]-(+)-PHNO is an agonist radiotracer for $D_{2/3}R$ which also has preferential affinity for D_3R over D_2R [Narendran et al., 2006; Wilson et al., 2005]. This unique property of [^{11}C]-(+)-PHNO, ~20–40 fold selectivity of D_3R over D_2R [Freedman et al., 1994; Gallezot et al., 2012; Rabiner et al., 2009; Searle et al., 2010; Seeman et al., 1993], results in a differential contribution of D_2R and D_3R to the [^{11}C]-(+)-PHNO signal across different regions of interest (ROIs). The estimated percent of the [^{11}C]-(+)-PHNO signal attributed to D_3R across ROIs in humans are: substantia nigra (~100%), globus pallidus (GP, ~65%), ventral striatum (VS, ~26%), and dorsal caudate-putamen (negligible) [Graff-Guerrero et al., 2010; Searle et al., 2013b; Tziortzi et al., 2011]. Also, as an agonist, baseline [^{11}C]-(+)-PHNO binding to $D_{2/3}R$ is more sensitive to competition with endogenous dopamine in vivo in humans [Caravaggio et al., 2014, 2016a; Shotbolt et al., 2012]. Thus, it remains unknown how $D_{2/3}R$ availability measured with an agonist radiotracer, and how D_3R availability specifically, may be related to brain morphology.

In the current investigation, we sought to explore how $D_{2/3}R$ availability measured with the antagonist radiotracer [^{11}C]-raclopride and the agonist radiotracer [^{11}C]-

(+)-PHNO is related to subcortical brain volume in healthy persons. We specifically examined the volume of (i) striatal subdivisions, (ii) hippocampal subdivisions, (iii) thalamic subdivisions, and (iv) the amygdala. This investigation marks an important first step in elucidating how in vivo differences in dopaminergic functioning may relate to subcortical brain morphology. A better understanding of these relationships will help inform the use of neurochemical and structural brain changes as potential biomarkers for neuropsychiatric disease.

METHODS

Participants

Healthy control data from a previous study were reanalyzed for the current investigation [Nakajima et al., 2015]. This sample comprises data collected by our laboratory from various PET studies [Caravaggio et al., 2015b; Graff-Guerrero et al., 2008, 2009; Payer et al., 2014] that were approved by the Research Ethics Board of the Centre for Addiction and Mental Health (CAMH), Toronto. For the current investigation, subjects were included if they provided a T1 structural MRI (1.5T or 3T), and an [^{11}C]-raclopride or [^{11}C]-(+)-PHNO scan. The participants were right-handed and free of any major medical or psychiatric disorder as determined by clinical interview, the Mini-International Neuropsychiatric Interview, and electrocardiography. Current or past alcohol abuse was an exclusion criteria. Participants were required to provide a full urine drug screen, and produced a negative urine screen for drugs of abuse and/or pregnancy at inclusion and before the PET scan. This included ethyl alcohol. Before the scan, the aural temperature and blood pressure of the participants were measured to insure they were within normal limits. All participants provided written informed consent and were non-smokers.

MRI Imaging

Fifty-one subjects scanned with [^{11}C]-raclopride and 58 subjects scanned with [^{11}C]-(+)-PHNO provided fast spin echo T1-weighted imaging (fast spoiled gradient echo, TE = 5.3–15 ms, TR = 8.9–12 ms, FOV = 20 cm 3D, 256 × 256, voxel 1.5 mm isotropic, NEX = 1) acquired on a 1.5-Tesla Sigma-GE scanner (General Electric Medical Systems, Milwaukee, WI) at Toronto General Hospital (Toronto, Canada). Eleven subjects scanned with [^{11}C]-raclopride and 11 subjects scanned with [^{11}C]-(+)-PHNO underwent MRI fast spin echo T1-weighted imaging (TR/TE = 30/8 ms, flip angle 45°, field of view 24 cm, 256 × 256 matrix, 124 coronal slices, and slice thickness = 1.0 mm, NEX = 1) acquired on a 3-Tesla Signa-GE scanner (GE Discovery MR750 3T; 8-Channel Head Coil, GE Standard 8HR Brain) at CAMH (Toronto, Canada).

Subcortical Volume Analyses

The Multiple Automatically Generated Templates (MAGeT-Brain) algorithm [Chakravarty et al., 2013; Pipitone et al., 2014] was used to provide fully-automated segmentation of striatal subdivisions [Chakravarty et al., 2006], hippocampal subdivisions [Pipitone et al., 2014; Winterburn et al., 2013], thalamic subdivisions [Chakravarty et al., 2006, 2008, 2009], and the amygdala [Treadway et al., 2015]. Typically, in a multi-atlas segmentation approach, manually drawn labels from atlases are warped (or propagated) into subject space by applying transformations estimated from non-linear image registration. Candidate labels from all atlas images are fused (via probabilistic segmentation techniques) to create a final segmentation. The goal of the MAGeT-Brain algorithm is to mitigate sources of error from such approaches including: (1) spurious non-linear registration or resampling errors (including partial volume effects [PVE] in label resampling), and (2) irreconcilable differences in neuroanatomy between the atlas and target images. The MAGeT-Brain algorithm is a modified multi-atlas segmentation technique, which uses a limited number of high-quality manually segmented atlases as an input to reduce bias and enhance segmentation accuracy. MAGeT-Brain propagates atlas segmentations to a template library, formed from a subset of target images, via transformations estimated by nonlinear image registration. The resulting segmentations are then propagated to each target image and fused using a label fusion method. Specifically, for those subjects who provided a 1.5T MRI, subsets of subjects scanned with [^{11}C]-raclopride ($n = 21$) and [^{11}C]-(+)-PHNO ($n = 21$) were used as template libraries through which the final segmentation was bootstrapped. All 11 subjects who provided a 3T MRI were used as a separate template. Templates were chosen based on representative subject characteristics [Schuetze et al., 2016]. Each subject in the template library was segmented through non-linear atlas-to-template registration followed by label propagation, yielding a unique definition of the subdivisions for each of the templates. The bootstrapping of the final segmentations through the template library results in candidate labels produced for each subject and labels are then fused using a majority vote to complete the segmentation process. Non-linear registration was performed using a version of the Automatic Normalization Tools (ANTS) registration technique [Avants et al., 2008] that is compatible with the minc toolkit (https://github.com/vfonov/mincANTS). Volumes (mm^3) from ROIs were averaged across hemispheres. It is important to note that regional BP_{ND} values and regional volume values are not derived from images warped into the same space. Namely, the BP_{ND} values come from images normalized to MNI space, while the regional volume values do not (labels are propagated into individual subject space, based on a voxel-voting procedure from a large number of candidate labels, using study sample specific templates). Thus, it is highly unlikely that there is overlap in potential variance from differences in "goodness" of

TABLE I. Relationship between [^{11}C]-raclopride BP_{ND} and striatal volume in healthy participants ($n = 62$), controlling for age, sex, and total brain volume

	[^{11}C]-raclopride BP_{ND}			
Striatal Volume	Dorsal caudate	Dorsal putamen	Ventral striatum	Globus pallidus
Pre-commissural caudate	0.12	0.02	0.003	0.02
	(0.36)	(0.86)	(0.98)	(0.87)
Post-commissural caudate	0.08	−0.07	−0.09	0.02
	(0.57)	(0.61)	(0.52)	(0.88)
Pre-commissural putamen	0.15	0.16	0.08	−0.06
	(0.27)	(0.23)	(0.55)	(0.67)
Post-commissural putamen	0.19	0.16	0.06	−0.004
	(0.15)	(0.24)	(0.68)	(0.94)
Ventral striatum	0.23	0.19	**0.30**[a]	−0.02
	(0.08)	(0.16)	**(0.02)**	(0.87)
Globus pallidus	0.14	0.06	−0.04	−0.06
	(0.29)	(0.67)	(0.76)	(0.65)

Data are presented as Pearson product moment partial correlations (r) with P-values in parentheses.
[a]Significance at $P < 0.05$ (two-tailed), uncorrected for multiple comparisons (adjusted P-threshold < 0.002).

normalization to the same image space (MNI). Importantly, compared to other automated techniques such as FreeSurfer and FSL, MAGeT-Brain demonstrates the highest correlation with gold-standard manual segmentation techniques—FreeSurfer and FSL significantly overestimate subcortical volumes compared to MAGeT-Brain [Makowski et al., in press].

Total Brain Volume Analysis

The procedure for total brain volume (TBV) analysis has been published elsewhere [Plitman et al., 2016b]. TBV was obtained using the Brain Extraction based on non-local Segmentation Technique (BEaST) method [Eskildsen et al., 2012], which is based on non-local segmentation in a multi-resolution framework. Each voxel is labeled based on the similarity of its neighborhood of voxels to all the neighborhoods in a library of pre-defined priors, and a non-local means estimator is used to estimate the label at the voxel. Inputs are down-sampled to a lower resolution, segmentation is performed, and results are propagated up to higher resolutions [Eskildsen et al., 2012]. BEaST is designed to include CSF (in the ventricles, cerebellar cistern, deep sulci, along surface of brain, and brainstem), the brainstem, and cerebellar white matter (WM) and GM in the brain mask, while excluding the skull, skin, fat, muscles, dura, eyes, bone, exterior blood vessels, and exterior nerves.

PET Imaging

Subjects were asked to abstain from food for no less than 90 min prior to PET procedures. The radiosynthesis of [^{11}C]-raclopride [Wilson et al., 2000] and [^{11}C]-(+)-PHNO [Wilson et al., 2005], along with the acquisition of PET images [Graff-Guerrero et al., 2010], has been described in detail elsewhere. Images were acquired on a high–resolution, head-dedicated PET camera system (CPS-HRRT; Siemens Molecular Imaging, USA), which measures radioactivity in 207 brain slices with a thickness of 1.2 mm each. The in-plane resolution was ∼2.8 mm full-width at half-maximum (FWHM). Transmission scans were acquired with the use of a ^{137}Cs ($T_{1/2} = 30.2$ years, energy = 662 KeV) single-photon point source to provide attenuation correction, and the emission data were acquired in list mode. The raw data were reconstructed by filtered back-projection. For the [^{11}C]-raclopride scans ($n = 62$), the mean radioactivity dose was 9.75(±1.0)mCi, with a specific activity of 1,234.58(±569.11)mCi/μmol, and an injected mass of 3.78(±2.19)μg. [^{11}C]-raclopride data were acquired for 60 min and redefined into 28 frames (1–5 of 1-min duration, 6–25 of 2-min duration, and 26–28 of 5-min duration). For the [^{11}C]-(+)-PHNO scans ($n = 68$), the mean radioactivity dose was 9.13(±1.46)mCi, with a specific activity of 1,100.91(±394.67)mCi/μmol, and an injected mass of 2.15(±.47)μg. None of the participants included in this sample reported nausea given the [^{11}C]-(+)-PHNO injection. [^{11}C]-(+)-PHNO data were acquired for 90 min after injection and redefined into 30 frames (1–15 of 1–min duration and 16–30 of 5–min duration).

PET Image Analysis

The ROI-based analysis for [^{11}C]-(+)-PHNO has been described in detail elsewhere [Graff-Guerrero et al., 2008; Tziortzi et al., 2011]. Time activity curves (TACs) from ROIs were obtained from the dynamic PET images in native space with reference to each subject's co-registered MRI image. The co-registration of each subjects MRI to PET space was done using the normalized mutual

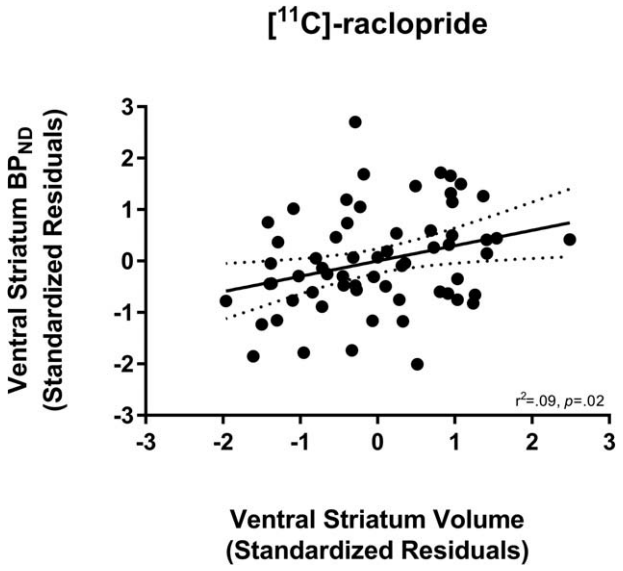

Figure 1.
Relationship between [^{11}C]-raclopride BP_{ND} in the ventral striatum (VS) and VS volume. Values represent standardized residuals controlling for age, sex, and total brain volume.

information algorithm [Studholme et al., 1997] as implemented in SPM2 (SPM2, Wellcome Department of Cognitive Neurology, London; http://www.fil.ion.ucl.ac.uk/spm). The TACs were analyzed using the Simplified Reference Tissue Method (SRTM) [Lammertsma and Hume, 1996] which has been validated for use with [^{11}C]-(+)-PHNO [Ginovart et al., 2007]. The cerebellum was used as the reference region to derive a quantitative estimate of binding—binding potential relative to the non-displaceable compartment (BP_{ND})—as defined by the consensus nomenclature for in vivo imaging of reversibly binding radioligands [Innis et al., 2007]. The basis function implementation of the SRTM [Gunn et al., 1997] was applied to the dynamic PET images to generate parametric voxelwise BP_{ND} maps using PMOD (v2.7, PMOD Technologies, Zurich, Switzerland). These images were spatially normalized into MNI brain space by Nearest Neighbor Interpolation with a voxel size fixed in $2 \times 2 \times 2$ mm^3 using SPM2. Regional BP_{ND} estimates were then derived from ROIs defined in MNI space, except for the hypothalamus and ventral pallidum ROIs. The VS and dorsal striatum (dorsal caudate, hereafter caudate, and dorsal putamen, hereafter putamen) were defined according with the criteria of Mawlawi et al [Mawlawi et al., 2001]. The GP ROI was defined according to the criteria of Tziortzi et al [Tziortzi et al., 2011].

Statistical Analysis

Statistical analyses were conducted using IBM SPSS (v.20; Armonk, NY: IBM Corp) and GraphPad Prism (v.7.0; GraphPad Software, La Jolla California). The relationship between $D_{2/3}R$ availability and subcortical volume was explored using partial correlations (two-tailed), controlling for age, gender, and TBV. Four exploratory partial correlation matrices were conducted separately for [^{11}C]-raclopride and [^{11}C]-(+)-PHNO (i.e., eight in total). These explored the relationship between BP_{ND} in each ROI and volumes of, (i) striatal subdivisions, (ii) hippocampal subdivisions, (iii) thalamic subdivisions, and (iv) the amygdalaBonferroni correction for multiple comparisons was applied to each correlation matrix individually, and relationships surviving this threshold ($P < 0.05 \div n$, where

TABLE II. Relationship between [^{11}C]-(+)-PHNO BP_{ND} and striatal volume in healthy participants ($n = 69$), controlling for age, sex, and total brain volume

	[^{11}C]-(+)-PHNO BP_{ND}				
Striatal volume	Substantia nigra	Dorsal caudate	Dorsal putamen	Ventral striatum	Globus pallidus
Pre-commissural caudate	−0.05	**0.26**[a]	0.17	0.21	0.11
	(0.69)	**(0.04)**	(0.17)	(0.10)	(0.38)
Post-commissural caudate	−0.02	**0.40**[c]	**0.32**[a]	0.01	**0.38**[c]
	(0.90)	**(0.001)**	**(0.01)**	(0.92)	**(0.002)**
Pre-commissural putamen	0.14	0.03	0.24	**0.26**[a]	0.11
	(0.26)	(0.79)	(0.05)	**(0.04)**	(0.39)
Post-commissural putamen	0.22	0.05	0.23	0.09	**0.30**[a]
	(0.08)	(0.72)	(0.07)	(0.49)	**(0.02)**
Ventral striatum	0.16	−0.02	−0.005	**0.39**[c]	−0.01
	(0.22)	(0.87)	(0.97)	**(0.001)**	(0.93)
Globus pallidus	0.22	**0.26**[a]	0.24	0.18	**0.36**[b]
	(0.09)	**(0.04)**	(0.06)	(0.15)	**(0.004)**

Data are presented as Pearson product moment partial correlations (r) with P-values in parentheses.
[a]Significance at $P < 0.05$ (two-tailed), uncorrected for multiple comparisons (adjusted P-threshold < 0.002).
[b]Significance at $P < 0.01$ (two-tailed), uncorrected for multiple comparisons (adjusted P-threshold < 0.002).
[c]Survives correction for multiple comparisons (adjusted P-threshold < 0.002).

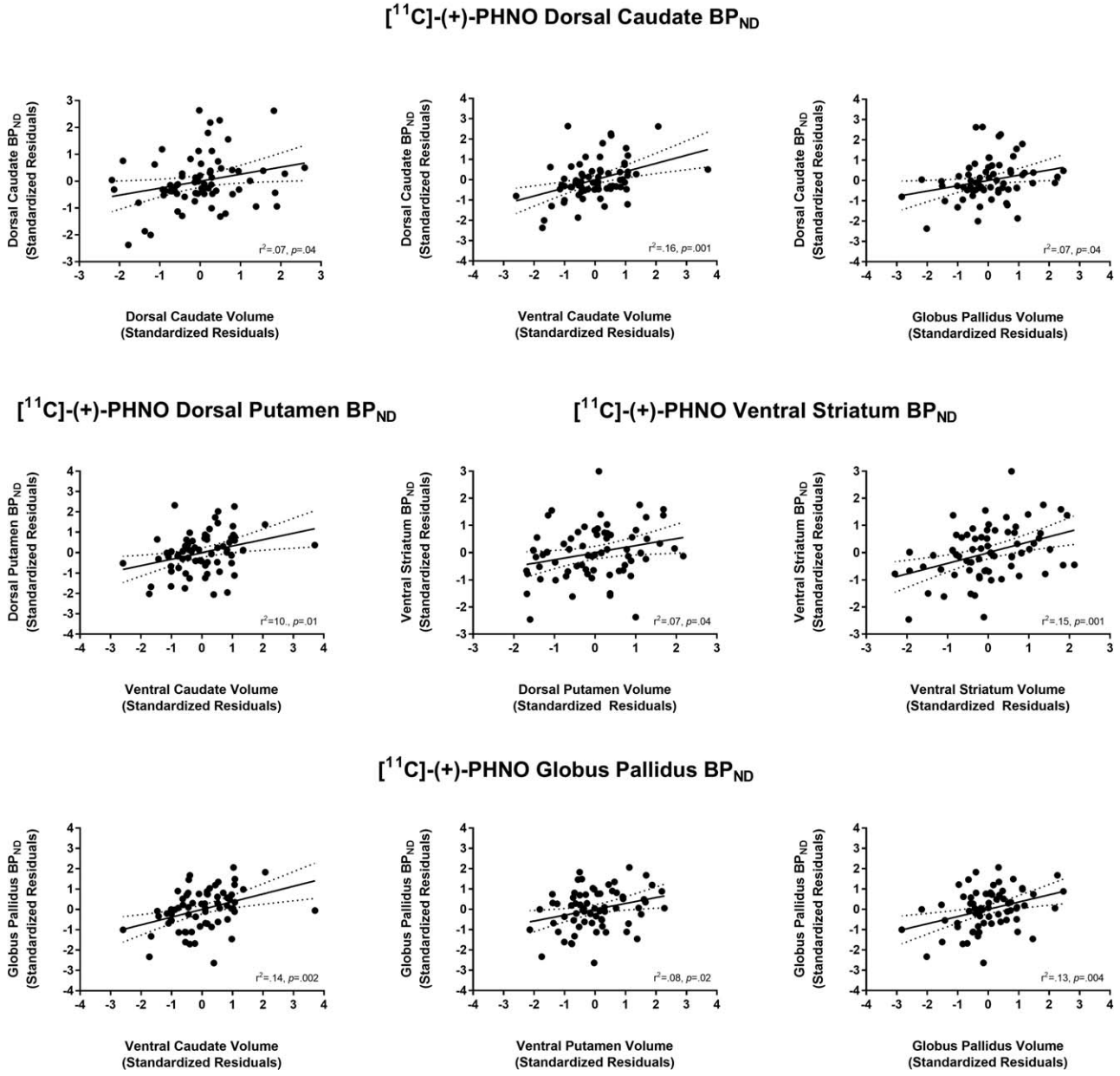

Figure 2.

Relationships between [^{11}C]-(+)-PHNO BP_{ND} in several regions of interest with striatal volumes. Values represent standardized residuals controlling for age, sex, and total brain volume.

n = # of comparisons) were considered noteworthy. We believe this exploratory, data-driven approach may help guide future studies in developing potential a priori hypotheses, while minimizing potential type-II errors.

RESULTS

Data from 62 subjects scanned with [^{11}C]-raclopride (mean age = 38.98 ± 14.45; 23 female) and 68 subjects scanned with [^{11}C]-(+)-PHNO (mean age = 38.54 ± 14.59; 25 female) were used in the study (see Supporting Information Figure 1). The relationships between striatal subregion volume and $D_{2/3}R$ availability measured with [^{11}C]-raclopride are presented in Table I. While [^{11}C]-raclopride BP_{ND} in the VS was positively correlated with VS volume (see Fig. 1), this relationship did not survive correction for multiple comparisons. Adding MRI fieldstrength (1.5T versus 3T) as an additional covariate did not significantly alter the strength of this finding ($r(56) = 0.30$, $P = 0.02$).

TABLE III. Relationship between [^{11}C]-raclopride BP_{ND} and hippocampal volume in healthy participants ($n = 62$), controlling for age, sex, and total brain volume

	[^{11}C]-raclopride BP_{ND}			
Hippocampal volume	Caudate	Putamen	Ventral striatum	Globus pallidus
CA1	−0.14	−0.17	−0.26	0.004
	(0.29)	(0.21)	(0.05)	(0.98)
Subiculum	0.003	−0.15	**–0.29**[a]	−0.02
	(0.98)	(0.25)	**(0.03)**	(0.90)
CA4/Dentate gyrus	−0.05	−0.02	−0.08	0.13
	(0.72)	(0.86)	(0.56)	(0.32)
CA2/CA3	−0.06	0.02	−0.06	0.09
	(0.67)	(0.88)	(0.64)	(0.48)
Stratum radiatum	−0.08	−0.13	−0.24	0.05
	(0.54)	(0.33)	(0.07)	(0.68)

Data are presented as Pearson product moment partial correlations (r) with P-values in parentheses.
[a]Significance at $P < 0.05$ (two-tailed), uncorrected for multiple comparisons (adjusted P-threshold < 0.003).

The relationships between striatal subregion volume and $D_{2/3}R$ availability measured with [^{11}C]-(+)-PHNO are presented in Table II and Figure 2. Several positive correlations emerged and survived correction for multiple comparisons. Notably, (i) BP_{ND} in both the dorsal caudate and GP was correlated with ventral caudate volume and (ii) BP_{ND} in the VS was correlated with VS volume. Adding MRI tesla strength as an additional covariate did not significantly alter the strength of any of the aforementioned correlations: ventral caudate volume with BP_{ND} in the dorsal caudate ($r(62) = 0.40$, $P = 0.001$) and GP ($r(62) = 0.38$, $P = 0.002$); VS volume with VS BP_{ND} ($r(62) = 0.39$, $P = 0.001$).

The relationships between hippocampal subregion volume and $D_{2/3}R$ availability measured with [^{11}C]-raclopride and [^{11}C]-(+)-PHNO are presented in Table III and Table IV, respectively. A negative correlation between [^{11}C]-raclopride BP_{ND} in the VS and subiculum volume was observed (see Fig. 3). However, this did not survive correction for multiple comparisons. Adding MRI tesla strength as an additional covariate did not significantly alter the strength of any of the aforementioned correlations: VS BP_{ND} with subiculum volume ($r(56) = -0.27$, $P = 0.04$).

The relationships between thalamic subregion volume and $D_{2/3}R$ availability measured with [^{11}C]-raclopride and [^{11}C]-(+)-PHNO and are presented in Table V and Table VI, respectively. While several positive and negative correlations emerged (see Fig. 4), none survived correction for multiple comparisons. Adding MRI tesla strength as an additional covariate did not significantly alter the strength of these correlations (data not shown).

For [^{11}C]-raclopride, amygdala volume was not significantly correlated with BP_{ND} in the caudate ($r(57) = -0.11$, $P = 0.45$), putamen ($r(57) = -0.06$, $P = 0.65$), VS ($r(57) = -0.11$, $P = 0.40$), nor the GP ($r(57) = 0.11$, $P = 0.41$). Adding

TABLE IV. Relationship between [^{11}C]-(+)-PHNO BP_{ND} and hippocampal volume in healthy participants ($n = 69$), controlling for age, sex, and total brain volume

	[^{11}C]-(+)-PHNO BP_{ND}				
Hippocampal volume	Substantia nigra	Caudate	Putamen	Ventral striatum	Globus pallidus
CA1	0.04	0.03	0.03	−0.11	0.11
	(0.76)	(0.79)	(0.79)	(0.37)	(0.38)
Subiculum	0.13	0.19	0.10	0.05	0.12
	(0.29)	(0.13)	(0.44)	(0.71)	(0.35)
CA4/Dentate gyrus	0.13	0.09	0.09	0.11	0.04
	(0.30)	(0.48)	(0.49)	(0.38)	(0.76)
CA2/CA3	0.13	−0.14	−0.08	0.01	0.10
	(0.30)	(0.26)	(0.55)	(0.91)	(0.41)
Stratum radiatum	0.04	−0.06	−0.03	−0.11	0.05
	(0.74)	(0.66)	(0.79)	(0.38)	(0.72)

Data are presented as Pearson product moment partial correlations (r) with P-values in parentheses.

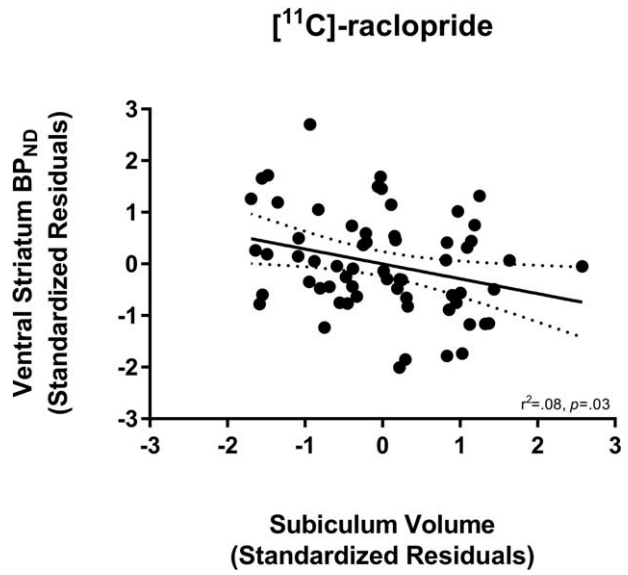

Figure 3.
Relationship between [^{11}C]-raclopride BP_{ND} in the ventral striatum (VS) and subiculum volume. Values represent standardized residuals controlling for age, sex, and total brain volume.

MRI tesla strength as an additional covariate did not significantly alter the strength of these correlations: caudate ($r(56) = -0.11$, $P = 0.40$), putamen ($r(56) = -0.05$, $P = 0.73$), VS ($r(56) = -0.09$, $P = 0.52$), and GP ($r(56) = 0.14$, $P = 0.23$). For [^{11}C]-(+)-PHNO, amygdala volume was not significantly correlated with BP_{ND} in the SN ($r(63) = 0.15$, $P = 0.24$), caudate ($r(63) = 0.14$, $P = 0.26$), putamen ($r(63) = 0.13$, $P = 0.30$), VS ($r(63) = 0.05$, $P = 0.72$), nor the GP ($r(63) = 0.12$, $P = 0.34$). Adding MRI tesla strength as an additional covariate did not significantly alter the strength of these correlations: SN ($r(62) = 0.15$, $P = 0.25$), caudate ($r(62) = 0.14$, $P = 0.26$), putamen ($r(62) = 0.12$, $P = 0.35$), VS ($r(62) = 0.05$, $P = 0.68$), and GP ($r(62) = 0.12$, $P = 0.36$).

DISCUSSION

This investigation is the first to examine how subcortical brain morphology is related to striatal D_2R and D_3R availability as measured with both an antagonist and agonist radiotracer. First with the antagonist [^{11}C]-raclopride, $D_{2/3}R$ availability within striatal subregions was generally not significantly correlated with the volume of those regions. This is in contrast to the findings of Woodward et al., who

TABLE V. Relationship between [^{11}C]-raclopride BP_{ND} and thalamus volume in healthy participants ($n = 62$), controlling for age, sex, and total brain volume

	[^{11}C]-raclopride BP_{ND}			
Thalamus volume	Caudate	Putamen	Ventral striatum	Globus pallidus
Lateral geniculate nucleus (LGN)	−0.21	**−0.30**[a]	−0.26	−0.14
	(0.13)	**(0.02)**	(0.05)	(0.30)
Medial geniculate nucleus (MGN)	−0.06	−0.11	−0.12	−0.12
	(0.68)	(0.40)	(0.35)	(0.36)
Anterior nuclei	−0.14	0.11	**0.29**[a]	0.09
	(0.30)	(0.41)	**(0.03)**	(0.48)
Central nuclei	0.02	−0.18	−0.24	−0.17
	(0.89)	(0.18)	(0.07)	(0.19)
Lateral dorsal	−0.04	0.10	0.15	−0.06
	(0.78)	(0.46)	(0.27)	(0.64)
Lateral posterior	−0.15	−0.07	−0.09	**−0.36**[a]
	(0.25)	(0.58)	(0.50)	**(0.006)**
Medial dorsal	0.02	0.01	−0.06	−0.06
	(0.86)	(0.93)	(0.68)	(0.67)
Pulvinar	−0.09	−0.09	−0.13	−0.08
	(0.51)	(0.52)	(0.31)	(0.55)
Ventral anterior nucleus (VAN)	−0.06	0.08	0.09	0.04
	(0.65)	(0.53)	(0.49)	(0.78)
Ventral lateral nucleus (VLN)	−0.03	−0.001	−0.04	−0.14
	(0.81)	(0.99)	(0.79)	(0.30)
Ventral posterior nucleus (VPN)	−0.03	−0.17	−0.18	−0.25
	(0.82)	(0.19)	(0.18)	(0.06)

Data are presented as Pearson product moment partial correlations (r) with P-values in parentheses.
[a]Significance at $P < 0.05$ (two-tailed), uncorrected for multiple comparisons (adjusted P-threshold < 0.001).

TABLE VI. Relationship between [^{11}C]-(+)-PHNO BP_{ND} and thalamus volume in healthy participants ($n = 67$), controlling for age, sex, and total brain volume

	[^{11}C]-(+)-PHNO BP_{ND}				
Thalamus volume	Substantia nigra	Caudate	Putamen	Ventral striatum	Globus pallidus
Lateral geniculate nucleus (LGN)	0.07	−0.003	−0.07	−0.09	0.02
	(0.57)	(0.98)	(0.58)	(0.49)	(0.87)
Medial geniculate nucleus (MGN)	0.11	0.002	−0.09	0.02	−0.11
	(0.39)	(0.99)	(0.48)	(0.91)	(0.37)
Anterior nuclei	−0.02	−0.001	0.03	0.19	−0.12
	(0.90)	(0.99)	(0.83)	(0.13)	(0.33)
Central nuclei	**0.26**[a]	−0.10	−0.01	0.19	−0.08
	(0.04)	(0.42)	(0.93)	(0.12)	(0.52)
Lateral dorsal	−0.08	0.09	0.05	0.14	−0.005
	(0.52)	(0.48)	(0.68)	(0.27)	(0.97)
Lateral posterior	−0.07	−0.03	−0.05	0.05	−0.19
	(0.60)	(0.85)	(0.70)	(0.69)	(0.14)
Medial dorsal	−0.07	−0.20	0.03	0.16	−0.07
	(0.56)	(0.12)	(0.81)	(0.20)	(0.58)
Pulvinar	0.02	−0.10	0.04	−0.09	0.06
	(0.90)	(0.45)	(0.77)	(0.50)	(0.62)
Ventral anterior nucleus (VAN)	−0.03	−0.02	0.02	**0.26**[a]	−0.13
	(0.83)	(0.86)	(0.86)	**(0.04)**	(0.30)
Ventral lateral nucleus (VLN)	−0.04	−0.03	0.02	0.18	−0.14
	(0.73)	(0.82)	(0.87)	(0.14)	(0.27)
Ventral posterior nucleus (VPN)	0.06	0.03	0.03	−0.02	−0.05
	(0.62)	(0.84)	(0.79)	(0.86)	(0.67)

Data are presented as Pearson product moment partial correlations (r) with P-values in parentheses.
[a]Significance at $P < 0.05$ (two-tailed), uncorrected for multiple comparisons (adjusted P-threshold < 0.001).

used the antagonist radiotracer [^{18}F]-fallypride [Woodward et al., 2009]. One exception was the VS, for which there was a positive correlation that did not survive correction for multiple comparisons. However, with the agonist [^{11}C]-(+)-PHNO, BP_{ND} within striatal subregions was generally correlated with the volume of those regions, with the exception of the putamen. Notably, this was especially true for the VS, which survived correction for multiple comparisons.

One potential interpretation of this finding is a causal, biological one. Namely, that the availability of functional $D_{2/3}R$ binding sites (i.e., D_2High) is positively related to striatal size, while the availability of total binding sites (i.e., $D_2High + D_2Low$) is not. As [^{11}C]-(+)-PHNO is more sensitive to endogenous DA at baseline [Caravaggio et al., 2016a], an alternative interpretation is that persons with less endogenous DA (and therefore more radiotracer binding) have larger striatal volumes. Another potential interpretation is a methodological one. Namely, that subtle individual variations in striatal size which persist after normalization may influence $D_{2/3}R$ availability measures, that is, a partial volume effect (PVE). The PVE is a phenomenon whereby the apparent concentration of a radiotracer decreases as the size of the ROI approaches the instrument resolution (FWHM) [Hoffman et al., 1979]. We suggest it is unlikely that our findings are due to potential PVE. First, PVEs are most pronounced for ROIs 2–3 times smaller than the FWHM [Rousset et al., 1998]. It is also a concern for studies of aging, where certain ROIs are known to decrease in size with age. However, the PVE is minimized using the resolution of the CPS-HRRT, and we have not observed significant PVE using other radiotracers in healthy persons with this scanner [Nakajima et al., 2015; Uchida et al., 2011]. Moreover, it is unclear why [^{11}C]-(+)-PHNO BP_{ND} in the striatum would be more susceptible to PVE than [^{11}C]-raclopride, acquired on the same scanner.

Unlike Woodward et al. [2009], we controlled for differences in age, gender, and TBV. Thus, our findings suggest that after considering these factors, subtle variations in striatal structure may be related to $D_{2/3}R$ availability measured with [^{11}C]-(+)-PHNO, but not [^{11}C]-raclopride. This finding is generally important for [^{11}C]-(+)-PHNO studies using cross-sectional or between group designs. For example, it will be important to determine whether increased [^{11}C]-(+)-PHNO BP_{ND} in obese persons corresponds with concordant increases in striatal volumes [Caravaggio et al., 2015c; Gaiser et al., 2016].

Notably, [^{11}C]-(+)-PHNO BP_{ND} in the dorsal caudate and GP were both correlated with ventral caudate volume. As the dorsal and ventral caudate border each other, it could be argued that this relationship is being driven by spill-over effects. However, with such an interpretation it

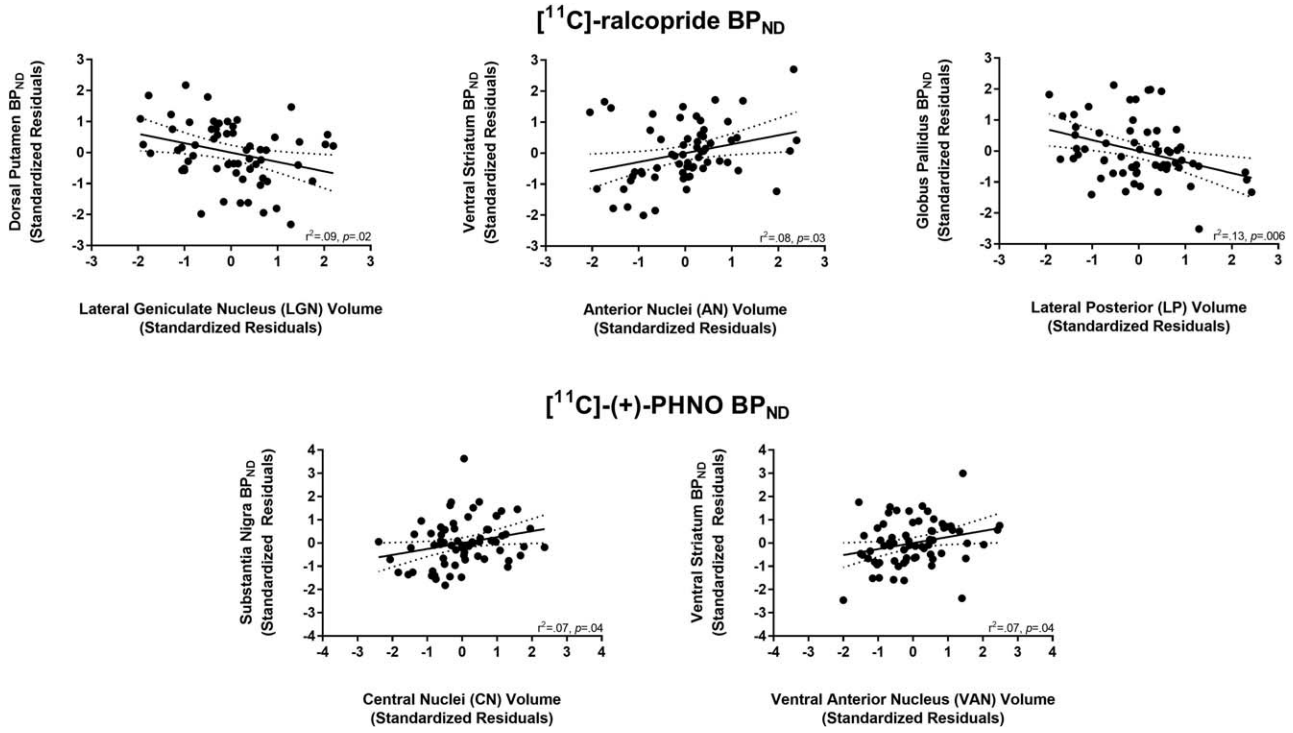

Figure 4.
Relationship between [^{11}C]-raclopride and [^{11}C]-(+)-PHNO BP_{ND} in several regions of interest with thalamic volumes. Values represent standardized residuals controlling for age, sex, and total brain volume.

would be harder to explain the relationship between GP BP_{ND} and ventral caudate volume. Notably, ~65% of the [^{11}C]-(+)-PHNO BP_{ND} signal from the GP reflects D_3R versus D_2R [Tziortzi et al., 2011]. While the dorsal caudate and putamen have negligible D_3R expression, the ventral caudate and putamen express D_3R (~$1/3^{rd}$) [Seeman et al., 2006]. It may be possible that neurons which express D_3R in the ventral caudate project to those neurons in the internal segment of the GP (GPi) which express D_3R [Gurevich and Joyce, 1999]. This in turn could potentially drive the relationship between [^{11}C]-(+)-PHNO BP_{ND} in the GP and ventral caudate volume. However, this is speculative and requires substantiation from ex vivo work.

We also explored how $D_{2/3}R$ availability in the striatum was related to the volume of other subcortical structures: the hippocampus, thalamus, and amygdala. While none of these correlations survived correction for multiple comparisons, a few notable relationships emerged. First, with [^{11}C]-raclopride there was a negative correlation between VS BP_{ND} and subiculum volume of the hippocampus. The subiculum, which is the main output structure of the hippocampus, projects densely to the nucleus accumbens of the VS [Chase et al., 2015; Groenewegen et al., 1987; Kelley and Domesick, 1982; Lopes da Silva et al., 1984]. It will be important for future in vivo and ex vivo work to elucidate the relationship between the structure and neurochemistry of this pathway. [^{11}C]-raclopride BP_{ND} in the GP was also negatively correlated with the volume of the lateral posterior nucleus of the thalamus. This large nucleus lies medial to the dorsal lateral geniculate nucleus and receives inputs mainly from the superior colliculus—projecting to primary and secondary visual areas [Puelles et al., 2012]. The superior colliculus plays a large role in integrating sensory motor information and, in particular, the generation of saccadic eye movements [Gandhi and Katnani, 2011]. Interestingly, while the GP is involved in motor generation and inhibition in general, the external segment of the GP (GPe) in particular may play an integral role in the generation and suppression of antisaccadic eye movements [Yoshida and Tanaka, 2016]. As the majority of the [^{11}C]-raclopride BP_{ND} in the GP reflects D_2R in the external segment, our exploratory finding may point to a role for these receptors in saccadic eye movements. While highly speculative, we surmise that future PET studies should examine the relationship between the availability of D_2R in the GPe and D_3R in the GPi and saccadic eye movements—measured with [^{11}C]-raclopride and [^{11}C]-(+)-PHNO, respectively.

There are several limitations to the current investigation. First, it has been noted that the injected mass of [^{11}C]-(+)-PHNO is not within ideal radiotracer conditions (i.e., <1.5 ng/kg) [Gallezot et al., 2012]. The specific activity required

to obtain tracer conditions is not possible with the available radiosynthesis method. While this limitation is currently unavoidable, we attempt to minimize this technical limitation by aiming to control the injected mass of the radiotracer to ≤2.5 μg (≤0.02 μg/kg), as previously used [Mizrahi et al., 2009; Rabiner and Laruelle, 2010; Searle et al., 2013a]. Importantly, our sample (mean injected mass: 2.15 ± 0.47μg) did not include any incidence of side effects associated with high [^{11}C]-(+)-PHNO injected mass, such as nausea/vomiting [Mizrahi et al., 2009; Rabiner and Laruelle, 2010]. Second, it has been suggested that [^{11}C]-(+)-PHNO BP_{ND} in D_3R-rich regions is underestimated if SRTM quantification is used in conjunction with 90 min of data acquisition [Girgis et al., 2011]. Thus, using arterial plasma-based kinetic models following 120 min of emission data is more ideal for quantifying [^{11}C]-(+)-PHNO BP_{ND} in D_3R-rich regions [Girgis et al., 2011]. Moreover, use of arterial plasma-based kinetic models would circumvent limitations associated with using reference tissue methods, namely concerns about specific binding to D_3R in cerebellar reference tissue [Searle et al., 2013b]. Future [^{11}C]-(+)-PHNO studies would benefit from examining the relationship between $D_{2/3}$R availability and brain morphology using plasma-based modeling and 120 mine emission data. This study was retrospective, reanalyzing previously collected PET data. Thus, other relevant measures such as cognition were not available. Moreover, it would be important to determine how longitudinal changes in $D_{2/3}$R availability with age may be associated with age-related changes in brain morphology in healthy persons and persons with neuropsychiatric disorders. Moreover, it will be important to determine how brain morphology changes and striatal $D_{2/3}$R availability changes relate to each other in addiction. For example, while we did not include heavy drinkers in our study, it would be important to determine how the frequency of alcohol use affects the relationship between in vivo brain morphology measures and DA measures. Finally, it will be important for future studies to examine how brain morphology is related to the in vivo status of other neurochemical systems. For example, increased striatal glutamate levels measured with proton magnetic resonance spectroscopy (^{1}H-MRS) have also been observed in patients with first-episode psychosis [Plitman et al., 2016a]. In turn, striatal glutamate levels were found to be negatively correlated with dorsal caudate volumes in these patients [Plitman et al., 2016b]. Given the potential interactions between striatal DA and glutamate [Caravaggio et al., 2016b; Stone et al., 2007], it can be inferred that the dopaminergic changes observed in schizophrenia may also be related changes in brain morphology. However, without direct evidence this remains merely conjuncture.

While our participants were not taking medications for any serious medical condition, we did not record oral contraceptive use in our female participants. While some [^{11}C]-raclopride PET studies have observed no effect of menstrual cycle on baseline $D_{2/3}$R availability in humans [Farde et al., 1995; Nordström et al., 1998], it is currently unknown whether this may effect [^{11}C]-(+)-PHNO BP_{ND}. Future studies are required to examine the potential interacting effects between menstrual cycle, contraceptive use, and the availability of $D_{2/3}$R using agonist radiotracers in females. Several lines of indirect evidence suggest that striatal DA functioning may differ between men and women. For example, women may be more vulnerable to the reinforcing effects of drugs of abuse [Becker and Hu, 2008; Fattore et al., 2007; Lynch et al., 2002; Nolen-Hoeksema, 2004]. However, PET studies in humans have provided conflicting results as to whether there are sex differences in amphetamine-induced striatal dopamine release [Munro et al., 2006; Riccardi et al., 2006, 2011]. Moreover, some studies suggest that DA transporter availability may not differ between gender, nor across the menstrual cycle [Best et al., 2005]. However, other studies suggests that women may have greater DA transporter functioning in the dorsal striatum [Andersen et al., 2012; Kaasinen et al., 2015; Lee et al., 2015; Wong et al., 2012], as well as greater DA synthesis capacity in the caudate [Laakso et al., 2002]. While we used sex as a covariate in our main analyses, there may be important sex differences between $D_{2/3}$R availability and brain morphology. For the purposes of transparency, in Supporting Information A, we re-conduct all our exploratory analyses within males and females separately. However, we did not sufficiently sample a large, nor equally matched number of males and females. Thus, interpretation of these data warrants caution and requires replication by sufficiently powered samples in the future.

Elucidating the relationship between metabolic health and striatal $D_{2/3}$R availability remains an on-going and exciting field of exploration in PET [Caravaggio et al., 2015a,c; Dang et al., 2016; Gaiser et al., 2016; Horstmann, 2017]. It is beyond the scope of the current manuscript to review all these conflicting PET findings; considering all the different radioligands used for $D_{2/3}$R, each with their own unique in vivo binding characteristics. Unfortunately, in our current sample, body mass index (BMI) was not collected for all the subjects. Moreover, other relevant markers of metabolic health, such as lipid profiles and insulin resistance, were not collected. In Supporting Information B, we provide the demographics of the subjects who provided BMI. For these subjects, we also re-ran all the analyses of the current investigation using BMI as an additional covariate. Notably, only four subjects scanned with [^{11}C]-raclopride and three subjects scanned with [^{11}C]-(+)-PHNO had BMI's within the moderately obese range (30–35). This is unsurprising as having a co-morbid medical condition, such as diabetes or heart disease, was an exclusion criteria for being scanned in this retrospective dataset. Thus, we warrant caution when interpreting these supplementary results. We believe our sample is inadequate to address how obesity modulates $D_{2/3}$R availability

and brain morphology; we present this Supporting Information for the purposes of transparency, and for guiding future studies which are better poised to address this important topic. Related to metabolic syndrome, several lines of evidence suggest that low-grade systemic inflammation may have an impact on cognition and brain structure [Marsland et al., 2015; Minihane et al., 2015]. While we have tried to screen "healthy" participants, we did not collect peripheral markers of inflammation. Future studies should examine how peripheral inflammatory markers—such as cytokines, leukocytes, and C-reactive protein levels—relates to concurrent changes in brain morphology and $D_{2/3}R$ availability; in healthy persons, persons with neuropsychiatric disorders, and persons with metabolic diseases.

In our sample, PET scans were collected at various times of day. Moreover, we did not record when was the last meal participants had before their PET scans and were only suggested to abstain from food for no less than 90 min prior to PET. To our knowledge, DA release in response to food intake has only been examined with [^{11}C]-raclopride, and methylphenidate was required to be co-administered to see a significant change in BP_{ND} [Volkow et al., 2002; Wang et al., 2011]. However, given the increased sensitivity of [^{11}C]-(+)-PHNO to DA release, this tracer may be able to quantify DA release in response to food receipt without the co-administration of methylphenidate. This can be examined by future [^{11}C]-(+)-PHNO studies. With regards to the current investigation, it is noteworthy that the time of day of the scan did not correlate with the BP_{ND} of [^{11}C]-(+)-PHNO (SN: $r = 0.09$, $P = 0.49$; Caudate: $r = 0.10$, $P = 0.43$; Putamen: $r = 0.009$, $P = 0.95$; VS: $r = 0.20$, $P = 0.11$; GP: $r = -0.15$, $P = 0.21$) nor of [^{11}C]-raclopride (Caudate: $r = 0.11$, $P = 0.41$; Putamen: $r = 0.11$, $P = 0.40$; VS: $r = 0.12$, $P = 0.36$; GP: $r = 0.03$, $P = 0.85$). Moreover, the month of scan acquisition was not correlated with the BP_{ND} of [^{11}C]- (+)-PHNO (SN: $r = -0.02$, $P = .86$; Caudate: $r = -0.07$, $P = 0.57$; Putamen: $r = 0.06$, $P = 0.63$; VS: $r = 0.04$, $P = 0.74$; GP: $r = 0.13$, $P = 0.29$) nor of [^{11}C]-raclopride (Caudate: $r = 0.02$, $P = 0.90$; Putamen: $r = -0.04$, $P = 0.79$; VS: $r = 0.04$, $P = 0.78$; GP: $r = -0.08$, $P = 0.53$). While the time of the last meal is not routinely collected across DA PET scans, this may be an important consideration for the future.

In sum, we examined how striatal $D_{2/3}R$ availability, measured with the antagonist [^{11}C]-raclopride and the agonist [^{11}C]-(+)-PHNO, was related to the volume of several subcortical structures in healthy controls. Such an exploration will, (1) aid the interpretation of future PET findings and (2) help elucidate the relationships between brain chemistry, structure, and function which could be used as potential biomarkers for neuropsychiatric disease. Extension of this work to understand how abnormal in vivo DA functioning relates to brain structure and function in disorders like schizophrenia and food addiction are highly warranted.

CONFLICT OF INTEREST

The authors have no potential conflicts of interest to declare in relation to the current study.

REFERENCES

Abi-Dargham A, Rodenhiser J, Printz D, Zea-Ponce Y, Gil R, Kegeles LS, Weiss R, Cooper TB, Mann JJ, Van Heertum RL, Gorman JM, Laruelle M (2000): Increased baseline occupancy of D2 receptors by dopamine in schizophrenia. Proc Natl Acad Sci USA 97:8104–8109.

Alvarez C, Vitalis T, Fon EA, Hanoun N, Hamon M, Seif I, Edwards R, Gaspar P, Cases O (2002): Effects of genetic depletion of monoamines on somatosensory cortical development. Neuroscience 115:753–764.

Andersen ML, Sawyer EK, Howell LL (2012): Contributions of neuroimaging to understanding sex differences in cocaine abuse. Exp Clin Psychopharmacol 20:2–15.

Avants BB, Epstein CL, Grossman M, Gee JC (2008): Symmetric diffeomorphic image registration with cross-correlation: Evaluating automated labeling of elderly and neurodegenerative brain. Med Image Anal 12:26–41.

Becker JB, Hu M (2008): Sex differences in drug abuse. Front Neuroendocrinol 29:36–47.

Best SE, Sarrel PM, Malison RT, Laruelle M, Zoghbi SS, Baldwin RM, Seibyl JP, Innis RB, van Dyck CH (2005): Striatal dopamine transporter availability with [123I]β-CIT SPECT is unrelated to gender or menstrual cycle. Psychopharmacology 183: 181–189.

Bond DJ, Lang DJ, Noronha MM, Kunz M, Torres IJ, Su W, Honer WG, Lam RW, Yatham LN (2011): The association of elevated body mass index with reduced brain volumes in first-episode mania. Biol Psychiatry 70:381–387.

Caravaggio F, Nakajima S, Borlido C, Remington G, Gerretsen P, Wilson A, Houle S, Menon M, Mamo D, Graff-Guerrero A (2014): Estimating endogenous dopamine levels at D2 and D3 receptors in humans using the agonist radiotracer [(11)C]-(+)-PHNO. Neuropsychopharmacology 39:2769–2776.

Caravaggio F, Borlido C, Hahn M, Feng Z, Fervaha G, Gerretsen P, Nakajima S, Plitman E, Chung JK, Iwata Y, Wilson A, Remington G, Graff-Guerrero A (2015a): Reduced insulin sensitivity is related to less endogenous dopamine at D2/3 receptors in the ventral striatum of healthy nonobese humans. Int J Neuropsychopharmacol 18:pyv014–pyv014.

Caravaggio F, Borlido C, Wilson A, Graff-Guerrero A (2015b): Examining endogenous dopamine in treated schizophrenia using [(1)(1)C]-(+)-PHNO positron emission tomography: A pilot study. Clin Chim Acta 449:60–62.

Caravaggio F, Raitsin S, Gerretsen P, Nakajima S, Wilson A, Graff-Guerrero A (2015c): Ventral striatum binding of a dopamine D2/3 receptor agonist but not antagonist predicts normal body mass index. Biol Psychiatry 77:196–202.

Caravaggio F, Kegeles LS, Wilson AA, Remington G, Borlido C, Mamo DC, Graff-Guerrero A (2016a): Estimating the effect of endogenous dopamine on baseline [(11) C]-(+)-PHNO binding in the human brain. Synapse (New York, N.Y.) 70:453–460.

Caravaggio F, Nakajima S, Plitman E, Gerretsen P, Chung JK, Iwata Y, Graff-Guerrero A (2016b): The effect of striatal dopamine depletion on striatal and cortical glutamate: A mini-review. Prog Neuropsychopharmacol Biol Psychiatry 65:49–53.

Casey KF, Cherkasova MV, Larcher K, Evans AC, Baker GB, Dagher A, Benkelfat C, Leyton M (2013): Individual differences in frontal cortical thickness correlate with the d-amphetamine-induced striatal dopamine response in humans. J Neurosci 33: 15285–15294.

Chakravarty MM, Bertrand G, Hodge CP, Sadikot AF, Collins DL (2006): The creation of a brain atlas for image guided neurosurgery using serial histological data. Neuroimage 30:359–376.

Chakravarty MM, Sadikot AF, Germann J, Bertrand G, Collins DL (2008): Towards a validation of atlas warping techniques. Med image Anal 12:713–726.

Chakravarty MM, Broadbent S, Rosa-Neto P, Lambert CM, Collins DL (2009): Design, construction, and validation of an MRI-compatible vibrotactile stimulator intended for clinical use. J Neurosci Methods 184:129–135.

Chakravarty MM, Steadman P, van Eede MC, Calcott RD, Gu V, Shaw P, Raznahan A, Collins DL, Lerch JP (2013): Performing label-fusion-based segmentation using multiple automatically generated templates. Hum Brain Mapp 34:2635–2654.

Chase HW, Clos M, Dibble S, Fox P, Grace AA, Phillips ML, Eickhoff SB (2015): Evidence for an anterior-posterior differentiation in the human hippocampal formation revealed by meta-analytic parcellation of fMRI coordinate maps: Focus on the subiculum. Neuroimage 113:44–60.

Dang LC, Samanez-Larkin GR, Castrellon JJ, Perkins SF, Cowan RL, Zald DH (2016): Associations between dopamine D2 receptor availability and BMI depend on age. NeuroImage 138: 176–183.

Ellison-Wright I, Glahn DC, Laird AR, Thelen SM, Bullmore E (2008): The anatomy of first-episode and chronic schizophrenia: An anatomical likelihood estimation meta-analysis. Am J Psychiatry 165:1015–1023.

Eskildsen SF, Coupe P, Fonov V, Manjon JV, Leung KK, Guizard N, Wassef SN, Ostergaard LR, Collins DL (2012): BEaST: Brain extraction based on nonlocal segmentation technique. Neuroimage 59:2362–2373.

Farde L, Hall H, Pauli S, Halldin C (1995): Variability in D2-dopamine receptor density and affinity: A PET study with [11C]raclopride in man. Synapse (New York, N.Y.) 20:200–208.

Fattore L, Altea S, Fratta W (2007): Sex differences in drug addiction: A review of animal and human studies. Womens Health 4:51–65.

Finnema SJ, Seneca N, Farde L, Shchukin E, Sovago J, Gulyas B, Wikstrom HV, Innis RB, Neumeyer JL, Halldin C (2005): A preliminary PET evaluation of the new dopamine D2 receptor agonist [11C]MNPA in cynomolgus monkey. Nucl Med Biol 32:353–360.

Freedman SB, Patel S, Marwood R, Emms F, Seabrook GR, Knowles MR, McAllister G (1994): Expression and pharmacological characterization of the human D3 dopamine receptor. J Pharmacol Exp Ther 268:417–426.

Gaiser EC, Gallezot J-D, Worhunsky PD, Jastreboff AM, Pittman B, Kantrovitz L, Angarita GA, Cosgrove KP, Potenza MN, Malison RT (2016): Elevated dopamine D2/3 receptor availability in obese individuals: A PET imaging study with [11C](+) PHNO. Neuropsychopharmacology 41:3042–3050.

Gallezot JD, Beaver JD, Gunn RN, Nabulsi N, Weinzimmer D, Singhal T, Slifstein M, Fowles K, Ding YS, Huang Y, Laruelle M, Carson RE, Rabiner EA (2012): Affinity and selectivity of [(1)(1)C]-(+)-PHNO for the D3 and D2 receptors in the rhesus monkey brain in vivo. Synapse (New York, N.Y.) 66:489–500.

Gandhi NJ, Katnani HA (2011): Motor functions of the superior colliculus. Annu Rev Neurosci 34:205–231.

Ginovart N, Willeit M, Rusjan P, Graff A, Bloomfield PM, Houle S, Kapur S, Wilson AA (2007): Positron emission tomography quantification of [11C]-(+)-PHNO binding in the human brain. J Cereb Blood Flow Metab 27:857–871.

Girgis RR, Xu X, Miyake N, Easwaramoorthy B, Gunn RN, Rabiner EA, Abi-Dargham A, Slifstein M (2011): In vivo binding of antipsychotics to D3 and D2 receptors: A PET study in baboons with [11C]-(+)-PHNO. Neuropsychopharmacology 36: 887–895.

Graff-Guerrero A, Willeit M, Ginovart N, Mamo D, Mizrahi R, Rusjan P, Vitcu I, Seeman P, Wilson AA, Kapur S (2008): Brain region binding of the D2/3 agonist [11C]-(+)-PHNO and the D2/3 antagonist [11C]raclopride in healthy humans. Hum Brain Mapp 29:400–410.

Graff-Guerrero A, Mamo D, Shammi CM, Mizrahi R, Marcon H, Barsoum P, Rusjan P, Houle S, Wilson AA, Kapur S (2009): The effect of antipsychotics on the high-affinity state of D2 and D3 receptors: A positron emission tomography study With [11C]-(+)-PHNO. Arch Gen Psychiatry 66:606–615.

Graff-Guerrero A, Redden L, Abi-Saab W, Katz DA, Houle S, Barsoum P, Bhathena A, Palaparthy R, Saltarelli MD, Kapur S (2010): Blockade of [11C](+)-PHNO binding in human subjects by the dopamine D3 receptor antagonist ABT-925. Int J Neuropsychopharmacol 13:273–287.

Groenewegen HJ, Vermeulen-Van der Zee E, te Kortschot A, Witter MP (1987): Organization of the projections from the subiculum to the ventral striatum in the rat. A study using anterograde transport of Phaseolus vulgaris leucoagglutinin. Neuroscience 23:103–120.

Gunn RN, Lammertsma AA, Hume SP, Cunningham VJ (1997): Parametric imaging of ligand-receptor binding in PET using a simplified reference region model. NeuroImage 6:279–287.

Guo J, Simmons WK, Herscovitch P, Martin A, Hall KD (2014): Striatal dopamine D2-like receptor correlation patterns with human obesity and opportunistic eating behavior. Mol Psychiatry 19:1078–1084.

Gurevich EV, Joyce JN (1999): Distribution of dopamine D3 receptor expressing neurons in the human forebrain: Comparison with D2 receptor expressing neurons. Neuropsychopharmacology 20:60–80.

Haijma SV, Van Haren N, Cahn W, Koolschijn PC, Hulshoff Pol HE, Kahn RS (2013): Brain volumes in schizophrenia: A meta-analysis in over 18 000 subjects. Schizophr Bull 39:1129–1138.

Hoffman EJ, Huang SC, Phelps ME (1979): Quantitation in positron emission computed tomography: 1. Effect of object size. J Comput Assist Tomogr 3:299–308.

Horstmann A (2017): It wasn't me; it was my brain – Obesity-associated characteristics of brain circuits governing decision-making. Physiol Behav 176:125–133.

Innis RB, Cunningham VJ, Delforge J, Fujita M, Gjedde A, Gunn RN, Holden J, Houle S, Huang SC, Ichise M, Iida H, Ito H, Kimura Y, Koeppe RA, Knudsen GM, Knuuti J, Lammertsma AA, Laruelle M, Logan J, Maguire RP, Mintun MA, Morris ED, Parsey R, Price JC, Slifstein M, Sossi V, Suhara T, Votaw JR, Wong DF, Carson RE (2007): Consensus nomenclature for in vivo imaging of reversibly binding radioligands. J Cereb Blood Flow Metab 27:1533–1539.

Jones L, Fischer I, Levitt P (1996): Nonuniform alteration of dendritic development in the cerebral cortex following prenatal cocaine exposure. Cereb Cortex (New York, N.Y.: 1991) 6:431–445.

Kaasinen V, Joutsa J, Noponen T, Johansson J, Seppanen M (2015): Effects of aging and gender on striatal and extrastriatal

[123I]FP-CIT binding in Parkinson's disease. Neurobiol Aging 36:1757–1763.

Kalsbeek A, Matthijssen MA, Uylings HB (1989): Morphometric analysis of prefrontal cortical development following neonatal lesioning of the dopaminergic mesocortical projection. Exp Brain Res 78:279–289.

Karlsson, H. (2016) Neuroreceptor Availability and Cerebral Morphology in Human Obesity. Turku, Finland: University of Turku.

Karlsson HK, Tuulari JJ, Tuominen L, Hirvonen J, Honka H, Parkkola R, Helin S, Salminen P, Nuutila P, Nummenmaa L (2016): Weight loss after bariatric surgery normalizes brain opioid receptors in morbid obesity. Mol Psychiatry 21:1057–1062.

Kegeles LS, Abi-Dargham A, Frankle WG, Gil R, Cooper TB, Slifstein M, Hwang DR, Huang Y, Haber SN, Laruelle M (2010): Increased synaptic dopamine function in associative regions of the striatum in schizophrenia. Arch Gen Psychiatry 67:231–239.

Kelley AE, Domesick VB (1982): The distribution of the projection from the hippocampal formation to the nucleus accumbens in the rat: An anterograde- and retrograde-horseradish peroxidase study. Neuroscience 7:2321–2335.

Laakso A, Vilkman H, Bergman J, Haaparanta M, Solin O, Syvalahti E, Salokangas RK, Hietala J (2002): Sex differences in striatal presynaptic dopamine synthesis capacity in healthy subjects. Biol Psychiatry 52:759–763.

Lammertsma AA, Hume SP (1996): Simplified reference tissue model for PET receptor studies. NeuroImage 4:153–158.

Lee JJ, Ham JH, Lee PH, Sohn YH (2015): Gender differences in age-related striatal dopamine depletion in Parkinson's disease. J Mov Disord 8:130–135.

Lopes da Silva FH, Arnolds DE, Neijt HC (1984): A functional link between the limbic cortex and ventral striatum: Physiology of the subiculum accumbens pathway. Exp Brain Res 55: 205–214.

Lynch WJ, Roth ME, Carroll ME (2002): Biological basis of sex differences in drug abuse: Preclinical and clinical studies. Psychopharmacology 164:121–137.

Makowski C, Beland S, Kostopoulos P, Bhagwat N, Devenyi GA, Malla AK, Joober R, Lepage M, Chakravarty MM (2017): Evaluating accuracy of striatal, pallidal, and thalamic segmentation methods: Comparing automated approaches to manual delineation. Neuroimage (in press).

Marsland AL, Gianaros PJ, Kuan DC, Sheu LK, Krajina K, Manuck SB (2015): Brain morphology links systemic inflammation to cognitive function in midlife adults. Brain Behav Immun 48:195–204.

Mawlawi O, Martinez D, Slifstein M, Broft A, Chatterjee R, Hwang DR, Huang Y, Simpson N, Ngo K, Van Heertum R, Laruelle M (2001): Imaging human mesolimbic dopamine transmission with positron emission tomography: I. Accuracy and precision of D(2) receptor parameter measurements in ventral striatum. J Cereb Blood Flow Metab 21:1034–1057.

Meredith G, Ypma P, Zahm D (1995): Effects of dopamine depletion on the morphology of medium spiny neurons in the shell and core of the rat nucleus accumbens. J Neurosci 15: 3808–3820.

Minihane AM, Vinoy S, Russell WR, Baka A, Roche HM, Tuohy KM, Teeling JL, Blaak EE, Fenech M, Vauzour D, McArdle HJ, Kremer BHA, Sterkman L, Vafeiadou K, Benedetti MM, Williams CM, Calder PC (2015): Low-grade inflammation, diet composition and health: Current research evidence and its translation. Br J Nutr 114:999–1012.

Mizrahi R, Wilson A, Houle S (2009): Side effects profile of [11C]-(+)-PHNO in human, a dopamine D2/3 agonist ligand. J Nucl Med 50:1288.

Morales AM, Kohno M, Robertson CL, Dean AC, Mandelkern MA, London ED (2015): Gray-matter volume, midbrain dopamine D2/D3 receptors and drug craving in methamphetamine users. Mol Psychiatry 20:764–771.

Munro CA, McCaul ME, Wong DF, Oswald LM, Zhou Y, Brasic J, Kuwabara H, Kumar A, Alexander M, Ye W, Wand GS (2006): Sex differences in striatal dopamine release in healthy adults. Biol Psychiatry 59:966–974.

Nakajima S, Caravaggio F, Boileau I, Chung JK, Plitman E, Gerretsen P, Wilson AA, Houle S, Mamo DC, Graff-Guerrero A (2015): Lack of age-dependent decrease in dopamine D(3) receptor availability: A [(11)C]-(+)-PHNO and [(11)C]-raclopride positron emission tomography study. J Cereb Blood Flow Metab 35:1812–1818.

Narendran R, Hwang DR, Slifstein M, Talbot PS, Erritzoe D, Huang Y, Cooper TB, Martinez D, Kegeles LS, Abi-Dargham A, Laruelle M (2004): In vivo vulnerability to competition by endogenous dopamine: Comparison of the D2 receptor agonist radiotracer (-)-N-[11C]propyl-norapomorphine ([11C]NPA) with the D2 receptor antagonist radiotracer [11C]-raclopride. Synapse (New York, N.Y.) 52:188–208.

Narendran R, Slifstein M, Guillin O, Hwang Y, Hwang DR, Scher E, Reeder S, Rabiner E, Laruelle M (2006): Dopamine (D2/3) receptor agonist positron emission tomography radiotracer [11C]-(+)-PHNO is a D3 receptor preferring agonist in vivo. Synapse (New York, N.Y.) 60:485–495.

Nolen-Hoeksema S (2004): Gender differences in risk factors and consequences for alcohol use and problems. Clin Psychol Rev 24:981–1010.

Nordström A-L, Olsson H, Halldin C (1998): A PET study of D2 dopamine receptor density at different phases of the menstrual cycle. Psychiatry Res 83:1–6.

Pappas BA, Murtha SJ, Park GA, Condon KT, Szirtes RM, Laventure SI, Ally A (1992): Neonatal brain dopamine depletion and the cortical and behavioral consequences of enriched postweaning environment. Pharmacol Biochem Behav 42: 741–748.

Payer DE, Behzadi A, Kish SJ, Houle S, Wilson AA, Rusjan PM, Tong J, Selby P, George TP, McCluskey T, Boileau I (2014): Heightened D3 dopamine receptor levels in cocaine dependence and contributions to the addiction behavioral phenotype: A positron emission tomography study with [11C]-+-PHNO. Neuropsychopharmacology 39:311–318.

Perlis RH (2011): Translating biomarkers to clinical practice. Mol Psychiatry 16:1076–1087.

Pipitone J, Park MT, Winterburn J, Lett TA, Lerch JP, Pruessner JC, Lepage M, Voineskos AN, Chakravarty MM (2014): Multi-atlas segmentation of the whole hippocampus and subfields using multiple automatically generated templates. Neuroimage 101:494–512.

Plitman E, de la Fuente-Sandoval C, Reyes-Madrigal F, Chavez S, Gomez-Cruz G, Leon-Ortiz P, Graff-Guerrero A (2016a): Elevated myo-inositol, choline, and glutamate levels in the associative striatum of antipsychotic-naive patients with first-episode psychosis: A proton magnetic resonance spectroscopy study with implications for glial dysfunction. Schizophr Bull 42:415–424.

Plitman E, Patel R, Chung JK, Pipitone J, Chavez S, Reyes-Madrigal F, Gomez-Cruz G, Leon-Ortiz P, Chakravarty MM,

de la Fuente-Sandoval C, Graff-Guerrero A (2016b): Glutamatergic metabolites, volume and cortical thickness in antipsychotic-naive patients with first-episode psychosis: Implications for excitotoxicity. Neuropsychopharmacology 41: 2606–2613.

Puelles, L., Martinez-de-la-Torre, M., Ferran, J.-L., Watson, C. (2012) Chapter 9 - Diencephalon. In: The Mouse Nervous System. San Diego: Academic Press. pp 313–336.

Rabiner EA, Laruelle M (2010): Imaging the D3 receptor in humans in vivo using [11C](+)-PHNO positron emission tomography (PET). Int J Neuropsychopharmacol 13:289–290.

Rabiner EA, Slifstein M, Nobrega J, Plisson C, Huiban M, Raymond R, Diwan M, Wilson AA, McCormick P, Gentile G, Gunn RN, Laruelle MA (2009): In vivo quantification of regional dopamine-D3 receptor binding potential of (+)-PHNO: Studies in non-human primates and transgenic mice. Synapse (New York, N.Y.) 63:782–793.

Reinoso BS, Undie AS, Levitt P (1996): Dopamine receptors mediate differential morphological effects on cerebral cortical neurons in vitro. J Neurosci Res 43:439–453.

Riccardi P, Zald D, Li R, Park S, Ansari MS, Dawant B, Anderson S, Woodward N, Schmidt D, Baldwin R, Kessler R (2006): Sex differences in amphetamine-induced displacement of [(18)F]fallypride in striatal and extrastriatal regions: A PET study. Am J Psychiatry 163:1639–1641.

Riccardi P, Park S, Anderson S, Doop M, Ansari M, Schmidt D, Baldwin R (2011): Sex Differences in the relationship of regional Dopamine release to affect and cognitive function in Striatal and Extrastriatal Regions using PET and [(18)F]Fallypride. Synapse (New York, N.Y.) 65:99–102.

Rimol LM, Hartberg CB, Nesvag R, Fennema-Notestine C, Hagler DJ, Jr., Pung CJ, Jennings RG, Haukvik UK, Lange E, Nakstad PH, Melle I, Andreassen OA, Dale AM, Agartz I (2010): Cortical thickness and subcortical volumes in schizophrenia and bipolar disorder. Biol Psychiatry 68:41–50.

Rousset OG, Ma Y, Evans AC (1998): Correction for partial volume effects in PET: Principle and validation. J Nucl Med 39: 904–911.

Schuetze M, Park MTM, Cho IYK, MacMaster FP, Chakravarty MM, Bray SL (2016): Morphological alterations in the thalamus, striatum, and pallidum in autism spectrum disorder. Neuropsychopharmacology 41:2627–2637.

Searle G, Beaver JD, Comley RA, Bani M, Tziortzi A, Slifstein M, Mugnaini M, Griffante C, Wilson AA, Merlo-Pich E, Houle S, Gunn R, Rabiner EA, Laruelle M (2010): Imaging dopamine D3 receptors in the human brain with positron emission tomography, [11C]PHNO, and a selective D3 receptor antagonist. Biol Psychiatry 68:392–399.

Searle GE, Beaver JD, Tziortzi A, Comley RA, Bani M, Ghibellini G, Merlo-Pich E, Rabiner EA, Laruelle M, Gunn RN (2013a): Mathematical modelling of [11C]-(+)-PHNO human competition studies. NeuroImage 68:119–132.

Searle GE, Beaver JD, Tziortzi A, Comley RA, Bani M, Ghibellini G, Merlo-Pich E, Rabiner EA, Laruelle M, Gunn RN (2013b): Mathematical modelling of [(1)(1)C]-(+)-PHNO human competition studies. Neuroimage 68:119–132.

Seeman P (2011): All roads to schizophrenia lead to dopamine supersensitivity and elevated dopamine D2(high) receptors. CNS Neurosci Ther 17:118–132.

Seeman P, Ulpian C, Larsen RD, Anderson PS (1993): Dopamine receptors labelled by PHNO. Synapse (New York, N.Y.) 14: 254–262.

Seeman P, Wilson A, Gmeiner P, Kapur S (2006): Dopamine D2 and D3 receptors in human putamen, caudate nucleus, and globus pallidus. Synapse (New York, N.Y.) 60:205–211.

Shotbolt P, Tziortzi AC, Searle GE, Colasanti A, van der Aart J, Abanades S, Plisson C, Miller SR, Huiban M, Beaver JD, Gunn RN, Laruelle M, Rabiner EA (2012): Within-subject comparison of [(11)C]-(+)-PHNO and [(11)C]raclopride sensitivity to acute amphetamine challenge in healthy humans. J Cereb Blood Flow Metab 32:127–136.

Song X, Quan M, Lv L, Li X, Pang L, Kennedy D, Hodge S, Harrington A, Ziedonis D, Fan X (2015): Decreased cortical thickness in drug naive first episode schizophrenia: In relation to serum levels of BDNF. J Psychiatric Res 60:22–28.

Stone JM, Morrison PD, Pilowsky LS (2007): Glutamate and dopamine dysregulation in schizophrenia–a synthesis and selective review. J Psychopharmacol (Oxford, England) 21:440–452.

Strimbu K, Tavel JA (2010): What are biomarkers? Curr Opin HIV AIDS 5:463–466.

Studholme C, Hill DL, Hawkes DJ (1997): Automated three-dimensional registration of magnetic resonance and positron emission tomography brain images by multiresolution optimization of voxel similarity measures. Med Phys 24:25–35.

Taki Y, Kinomura S, Sato K, Inoue K, Goto R, Okada K, Uchida S, Kawashima R, Fukuda H (2008): Relationship between body mass index and gray matter volume in 1,428 healthy individuals. Obesity (Silver Spring, Md.) 16:119–124.

Treadway MT, Waskom ML, Dillon DG, Holmes AJ, Park MT, Chakravarty MM, Dutra SJ, Polli FE, Iosifescu DV, Fava M, Gabrieli JD, Pizzagalli DA (2015): Illness progression, recent stress, and morphometry of hippocampal subfields and medial prefrontal cortex in major depression. Biol Psychiatry 77:285–294.

Tziortzi AC, Searle GE, Tzimopoulou S, Salinas C, Beaver JD, Jenkinson M, Laruelle M, Rabiner EA, Gunn RN (2011): Imaging dopamine receptors in humans with [11C]-(+)-PHNO: Dissection of D3 signal and anatomy. NeuroImage 54:264–277.

Uchida H, Chow TW, Mamo DC, Kapur S, Mulsant BH, Houle S, Pollock BG, Graff-Guerrero A (2011): Effects of aging on 5-HT(2A) R binding: A HRRT PET study with and without partial volume corrections. Int J Geriatr Psychiatry 26:1300–1308.

van Erp TG, Hibar DP, Rasmussen JM, Glahn DC, Pearlson GD, Andreassen OA, Agartz I, Westlye LT, Haukvik UK, Dale AM, Melle I, Hartberg CB, Gruber O, Kraemer B, Zilles D, Donohoe G, Kelly S, McDonald C, Morris DW, Cannon DM, Corvin A, Machielsen MW, Koenders L, de Haan L, Veltman DJ, Satterthwaite TD, Wolf DH, Gur RC, Gur RE, Potkin SG, Mathalon DH, Mueller BA, Preda A, Macciardi F, Ehrlich S, Walton E, Hass J, Calhoun VD, Bockholt HJ, Sponheim SR, Shoemaker JM, van Haren NE, Hulshoff Pol HE, Ophoff RA, Kahn RS, Roiz-Santianez R, Crespo-Facorro B, Wang L, Alpert KI, Jonsson EG, Dimitrova R, Bois C, Whalley HC, McIntosh AM, Lawrie SM, Hashimoto R, Thompson PM, Turner JA (2016): Subcortical brain volume abnormalities in 2028 individuals with schizophrenia and 2540 healthy controls via the ENIGMA consortium. Mol Psychiatry 21:547–553.

Veit R, Kullmann S, Heni M, Machann J, Häring H-U, Fritsche A, Preissl H (2014): Reduced cortical thickness associated with visceral fat and BMI. NeuroImage 6:307–311.

Volkow ND, Wang GJ, Fowler JS, Logan J, Jayne M, Franceschi D, Wong C, Gatley SJ, Gifford AN, Ding YS, Pappas N (2002): "Nonhedonic" food motivation in humans involves dopamine in the dorsal striatum and methylphenidate amplifies this effect. Synapse (New York, N.Y.) 44:175–180.

Walther K, Birdsill AC, Glisky EL, Ryan L (2010): Structural brain differences and cognitive functioning related to body mass index in older females. Hum Brain Mapp 31:1052–1064.

Wang GJ, Geliebter A, Volkow ND, Telang FW, Logan J, Jayne MC, Galanti K, Selig PA, Han H, Zhu W, Wong CT, Fowler JS (2011): Enhanced striatal dopamine release during food stimulation in binge eating disorder. Obesity (Silver Spring, Md.) 19:1601–1608.

Werhahn KJ, Landvogt C, Klimpe S, Buchholz HG, Yakushev I, Siessmeier T, Muller-Forell W, Piel M, Rosch F, Glaser M, Schreckenberger M, Bartenstein P (2006): Decreased dopamine D2/D3-receptor binding in temporal lobe epilepsy: An [18F]fallypride PET study. Epilepsia 47:1392–1396.

Willeit M, Ginovart N, Kapur S, Houle S, Hussey D, Seeman P, Wilson AA (2006): High-affinity states of human brain dopamine D2/3 receptors imaged by the agonist [11C]-(+)-PHNO. Biol Psychiatry 59:389–394.

Wilson AA, Garcia A, Jin L, Houle S (2000): Radiotracer synthesis from [(11)C]-iodomethane: A remarkably simple captive solvent method. Nucl Med Biol 27:529–532.

Wilson AA, McCormick P, Kapur S, Willeit M, Garcia A, Hussey D, Houle S, Seeman P, Ginovart N (2005): Radiosynthesis and evaluation of [11C]-(+)-4-propyl-3,4,4a,5,6,10b-hexahydro-2H-naphtho[1,2-b][1,4]oxazin-9-ol as a potential radiotracer for in vivo imaging of the dopamine D2 high-affinity state with positron emission tomography. J Med Chem 48:4153–4160.

Winterburn JL, Pruessner JC, Chavez S, Schira MM, Lobaugh NJ, Voineskos AN, Chakravarty MM (2013): A novel in vivo atlas of human hippocampal subfields using high-resolution 3 T magnetic resonance imaging. Neuroimage 74:254–265.

Wong KK, Muller ML, Kuwabara H, Studenski SA, Bohnen NI (2012): Gender differences in nigrostriatal dopaminergic innervation are present at young-to-middle but not at older age in normal adults. J Clin Neurosci 19:183–184.

Woodward ND, Zald DH, Ding Z, Riccardi P, Ansari MS, Baldwin RM, Cowan RL, Li R, Kessler RM (2009): Cerebral morphology and dopamine D2/D3 receptor distribution in humans: A combined [18F]fallypride and voxel-based morphometry study. Neuroimage 46:31–38.

Xiao Y, Lui S, Deng W, Yao L, Zhang W, Li S, Wu M, Xie T, He Y, Huang X, Hu J, Bi F, Li T, Gong Q (2015): Altered cortical thickness related to clinical severity but not the untreated disease duration in schizophrenia. Schizophr Bull 41:201–210.

Yoshida A, Tanaka M (2016): Two types of neurons in the primate globus pallidus external segment play distinct roles in antisaccade generation. Cereb Cortex (New York, N.Y.: 1991) 26: 1187–1199.